EPJ AP

Applied Physics

EPJ.org

your physics journal

Eur. Phys. J. Appl. Phys. (2014) 68: 30201 DOI: 10.1051/epjap/2014140272

Charge carrier trapping in highly-ordered lyotropic chromonic liquid crystal films based on ionic perylene diimide derivatives

Pavlo V. Soroka, Alexander Yu. Vakhnin, Yuriy A. Skryshevskiy, Oleksandr P. Boiko, Maksim I. Anisimov, Yuriy L. Slominskiy, Vassili G. Nazarenko, Jan Genoe, and Andrey Kadashchuk

edp sciences

The title “The European Physical Journal” is a joint property of EDP Sciences, Società Italiana di Fisica (SIF) and Springer

Eur. Phys. J. Appl. Phys. (2014) 68: 30201
DOI: 10.1051/epjap/2014140272

THE EUROPEAN PHYSICAL JOURNAL APPLIED PHYSICS

Regular Article

Charge carrier trapping in highly-ordered lyotropic chromonic liquid crystal films based on ionic perylene diimide derivatives

Pavlo V. Soroka[1], Alexander Yu. Vakhnin[1], Yuriy A. Skryshevskiy[1], Oleksandr P. Boiko[1,2], Maksim I. Anisimov[1], Yuriy L. Slominskiy[3], Vassili G. Nazarenko[1], Jan Genoe[4], and Andrey Kadashchuk[1,4,a]

[1] Institute of Physics, National Academy of Sciences of Ukraine, Prospect Nauky 46, 03028 Kyiv, Ukraine
[2] Center for Physical Sciences and Technology, Savanoriu 231, LT-02300 Vilnius, Lithuania
[3] Institute of Organic Chemistry, National Academy of Sciences of Ukraine, Murmanska 5, 02660 Kyiv, Ukraine
[4] IMEC, Kapeldreef 75, B-3001 Leuven, Belgium

Received: 1 July 2014 / Received in final form: 21 September 2014 / Accepted: 26 September 2014
Published online: 25 November 2014 –

Abstract. Charge carrier trapping in thin films of lyotropic chromonic liquid crystals (LCLCs) based on ionic perylene diimide derivative and in chemically-similar neutral N,N′-dipentyl-3,4,9,10-perylene-dicarboximide (PTCDI-C5) films is investigated by thermally-stimulated luminescence (TSL) technique. The LCLC films comprise elongated molecular aggregates featuring a long-range orientational order. The obtained results provide direct evidence for the improved energetic ordering (smaller effective energetic disorder) in aggregated LCLC films as compared to conventional PTCDI-C5 films. The width of the density-of-state distribution of 0.09 eV and 0.13 eV was estimated for the LCLC and PTCDI-C5 films, respectively. Relatively small effective energetic disorder in LCLC films is ascribed to formation of macroscopically larger LCLC aggregates.

1 Introduction

Organic semiconductor films offer a huge potential for the emerging flexible large-area electronics because they allow for a low-cost and low-temperature device fabrication compatible with flexible plastic substrates [1,2]. Organic electronic devices such as organic field-effect transistors (OFETs), light emitting diodes and solar cells or electrophotographic photoreceptors employed in today's photocopiers, are generally based upon non-crystalline systems such as vapor deposited molecular glasses consisting of small organic molecules or semiconducting polymers deposited from solutions. The charge-carrier mobility is one of the most important properties of organic semiconductors for their application in optoelectronics as it has a profound effect on ultimate device performance. The charge mobility in organic materials still remains by far lower than that of conventional inorganic semiconductors and, along with stability issue, makes a current bottleneck for the large scale industrial application of organic electronic devices.

It has been well established that *disorder* is a strong impact on that aspect of the device performance which is related to charge carrier mobility. This is caused by presence of significant energy disorder in the amorphous or polycrystalline semiconductor films which are commonly used nowadays in organic electronic devices [3–6]. Therefore the charge-carrier transport in such disordered materials occurs by thermally activated hopping [3–7] through a manifold of localized states with a density-of-state (DOS) distribution having an assumed Gaussian shape. This disorder, however, is not an inherent property of the organic semiconductors, but rather comes from the nature of the thin organic films conventionally prepared by deposition in vacuum or from solutions. Indeed, single-crystal organic semiconductors are known to possess much better characteristics and the high-performance electronic devices have been demonstrated for them [8–11]. Nowadays it became clear that charge transport properties of organic semiconductors are to large extent determined by molecular packing and macroscopic orientational ordering in thin films.

There are several approaches employed to-date to obtain highly-crystalline organic films. First, there were attempts to control growth of single crystallites locally by control of surface energy by self-assembled monolayers (SAM) using evaporation of organic semiconductors in vacuum [10] and also from solution [11]. Creation of oriented single-crystal arrays has been recently demonstrated by inkjet printing on SAM-controlled surfaces by Minemawari et al. [11]. Second, there are currently quite many studies of epitaxial growth of crystalline thin-films

[a] e-mail: kadash@iop.kiev.ua

of organic semiconductors on suitable template substrates. This approach started with epitaxial growth of molecular crystallites on selected templates such as mica [12–15]. Later on, organic-organic hetero-epitaxy was demonstrated and it was found that organic crystals can be oriented on another crystal even without perfect correspondence of lattice structure for the crystalline substrate and the growing hetero-crystal [16]. Although the organic "epitaxial" crystallites show ordering, they are most often of polycrystalline structure and not single crystals.

On the other hand, supramolecular assembly of the molecules in the solid state can be conveniently accomplished from nematic or smectic liquid crystal (LC) phases with or without the use of an additional orientation layer [8,9]. McCulloch et al. [17] demonstrated that liquid-crystalline materials with cross-linkable chemical bonds can be used as semiconductors in OFET devices. The idea behind this approach is an orientation of non-crosslinked compounds in the LC state followed by a final structural fixing of the ordered state by photochemical cross-linking. However, as pointed in [18], there are two serious limitations to these approaches: (i) alignment of monodomains with required orientation and size is challenging, and (ii) the structural and electronic properties in thermotropic LCs strongly depend on temperature because of the changing dynamics of molecules and because of the multiple phase transitions. The recent experiments with lyotropic chromonic liquid crystals (LCLC) [19] demonstrate some progress as the LCLC with their long-range orientational order, dense molecular packing and high flexibility of the structure in which the local defects do not dominate the local order and hence the global order introduced by deposition retains [20], offer an excellent potential alternative to the rigid crystals. In these materials the aromatic cores of the molecules are decorated with polar groups rather than aliphatic chains. These polar groups make the LCLC compound soluble in water. The strong $\pi - \pi$ interaction of the aromatic cores makes them stack on top of each other forming columnar aggregates [21]. The aggregate structure of LCLC prevents them from being tilted at the bounding substrate, thus the proper alignment is achieved without special aligning layers needed in the case of thermotropic LCs [20]. Subsequent drying "freezes" the highly aligned structure resulting in a solid film [22] with close packing of molecules along the aggregates with the same spacing of 0.34 nm as in the LC phase [23,24], but without imposing a long-range crystalline structure in the directions perpendicular to the aggregates.

Although the field-effect charge-carrier mobility measured for LCLC films was found to be relatively high (0.03 cm^2/V s) [19], there is no information about the energetic structure, the energy disorder and possible charge-carrier traps in solid LCLC films, which is very important for understanding of the electrical transport in molecular aggregates as well as for further device performance improvements. Trap detection techniques based on thermally-stimulated luminescence (TSL) and thermally-stimulated current (TSC) were demonstrated to be especially suitable for studying the charge-carrier traps (their energies and distribution) in disordered organic media [7,25–34] and allow the estimation of the width of the DOS distribution, σ (referred to as energetic disorder parameter). The TSL technique is of particular relevance due to it is a purely optical tool, which allows for separation of interface/contact effects and does not require good charge transport in the material. The TSL has been extensively applied by our group to study intrinsic energetic disorder in different organic semiconducting thin films including $\pi-$ and $\sigma-$conjugated polymers, molecularly doped polymers as well as small molecular weight oligomers [7,28–34]. In tandem with these studies, a firm theoretical background for application of TSL in disordered organic systems with hopping charge transport was also developed [28,31] using the concept of a thermally-stimulated carrier random walk within a positionally and energetically random system of hopping sites. In the present paper we apply the TSL method to study the charge-carrier trapping in self-organized perylene-based LCLC solid films and the results are compared with that obtained in films based on conventional perylene derivative PTCDI-C5 (see details below) having the same core structure.

2 Experimental methods

2.1 Materials

Molecular structures of the compounds used in this study are illustrated in Figures 1a and 1b. As a representative LCLC material we have studied a compound labeled hereafter as Per-2582SL (shown in Fig. 1a) which is an ionic perylene diimide derivative having the same core structure as a well-known *n*-channel OFET semiconductor N,N′-dipentyl-3,4,9,10-perylene-dicarboximide (PTCDI-C5) (Fig. 1b), but possesses different periphery groups containing ions. The LCLC material and PTCDI-C5 were synthesized at the Institute of Organic Chemistry (Kyiv) and used as received. The end ionic groups of the Per-2582SL dissociate in aqueous solution, while the planar cores of the molecules attract each other and stack on top of each other thanks to the intermolecular $\pi - \pi$ orbital interactions. The resulting aggregates are of columnar type as the planes of the molecules form stacks (rather than closed micelles common in amphiphilic systems). An aqueous solution of Per-2582SL (concentration of about 8 wt.%) was prepared in order to obtain a nematic phase [35]. The solution was deposited on a substrate and shear-aligned using the so-called "vertical" spin-coating technique (1500 rpm) [19,36]. The aligned films were dried at room temperature in air for several hours [35]. Thickness of the films prepared by our deposition technique was around 850 nm. The shear-aligned textures of solid films demonstrated uniform alignment characterized by a high dichroism and birefringence as shown in Figures 1c and 1d. UV-vis absorption spectra of the LCLC films have been presented before [37] along with detailed optical characterization of these films.

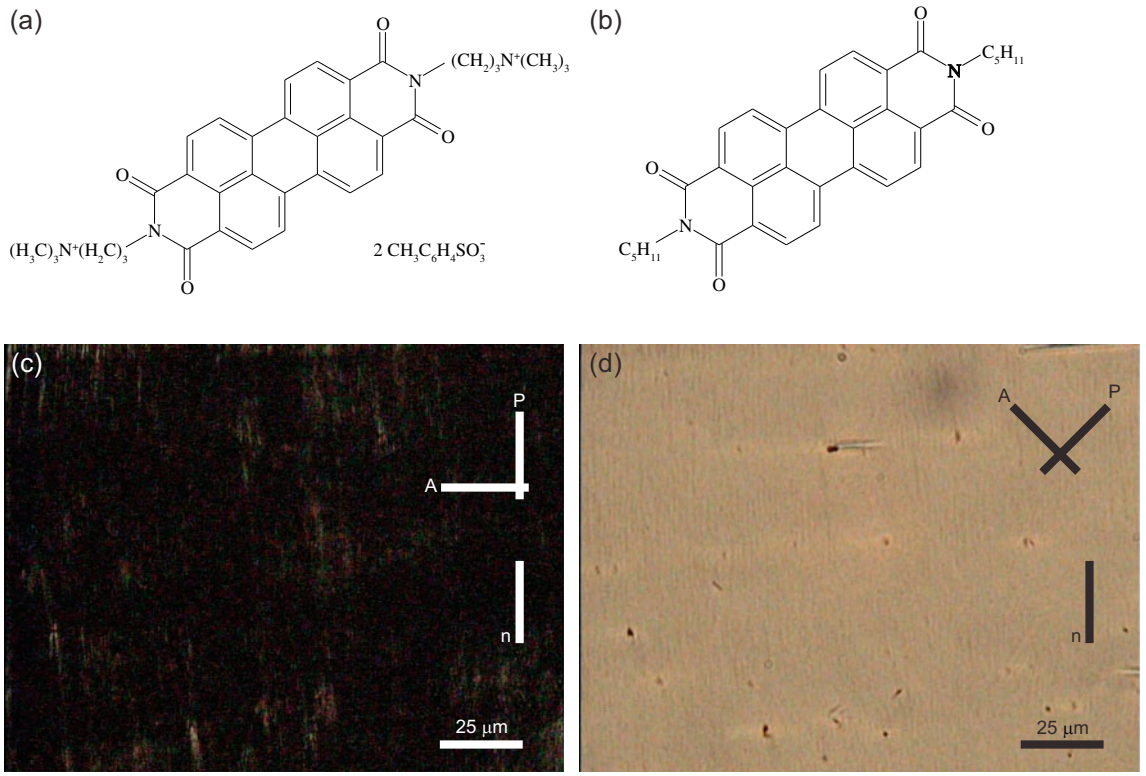

Fig. 1. Molecular structures of (a) Per-2582SL and (b) PTCDI-C5. Polarizing microscope textures of Per-2582SL films formed by vertical spin-coating: (c) and (d) differ in orientation of director (n) with respect to the polarizer (P) and analyzer (A).

For comparison purposes, the studies have also been performed for a neutral perylene diimide derivative PTCDI-C5 (Fig. 1b) which is a well-known organic semiconductor material used for fabrication of different organic electronic devices [38–40]. PTCDI-C5 has a similar core molecular structure as Per-2582SL, however, features no liquid crystalline properties. Deposited PTCDI-C5 form typically polycrystalline films with two nearly coplanar (stacked) molecules within the unit cell. The intermolecular distance along a-direction of PTCDI-C5 crystallite is relatively short, resulting in a large overlap of molecular $\pi-$orbitals, therefore this material is usually considered as a strongly coupled system. The OFET charge-carrier mobility in PTCDI-C5 films prepared by thermal evaporation was reported to be fairly large of about $\mu_e \approx 10^{-1}$ cm^2/V s [38] at room temperature and characterized by thermally-activated behavior with activation energies dependent on the gate voltage [38], that implies the presence of substantial energetic disorder in such films.

2.2 Experimental techniques

Thermally stimulated luminescence (TSL) is the phenomenon of luminescent emission after removal of excitation under conditions of increasing temperature. Generally, in the TSL method the trapping states are first populated by photogeneration of charge carriers, usually at low temperatures in order to prevent a fast escape. The trapped charge carriers are released by heating up the sample with a linear temperature ramp, while the luminescence due to radiative recombination is recorded as a function of temperature. TSL measurements were carried out with an automatic setup for optical thermally activational spectroscopy over a wide temperature range from 4.2 K to 350 K with an accuracy better than 0.1 K. The investigated samples were mounted in a holder of the optical helium cryostat and, after cooling, they were irradiated with UV light. For excitation, the light from a high-pressure 500 W mercury lamp was used. After terminating the excitation the luminescence signal was detected with a cooled photomultiplier operated in photon-counting mode. TSL measurements were performed in two different regimes; under the uniform heating with the rate $\beta = 0.15$ K/s and in the fractional heating regime [32,33].

The fractional TSL technique (also called the fractional glow technique), being a modulation version of thermally activational spectroscopy, is based on cycling the sample with a large number of small temperature oscillations superimposed on a constant heating ramp. This allows the determination of trap depth with high accuracy when different groups of traps are not well separated in energy or are continuously distributed, which is of special relevance for disordered organic solids. The low-temperature fractional TSL was applied to investigate the charge-carrier trapping in a great variety of important polymer and oligomer organic semiconductor materials

(see [7,25–34]). The mean activation energy $\langle E \rangle$ is determined during each temperature cycle as:

$$\langle E \rangle(T) = -\frac{\mathrm{d}[\ln I(T)]}{\mathrm{d}(1/kT)}, \quad (1)$$

where $I(T)$ is the intensity of the thermoluminescence, T is the temperature and k is the Boltzmann constant. Since a temperature oscillation, ΔT, is usually much less than mean value of T, the $\langle E \rangle$ could be assumed as equal to $E(T)$, the activation energy of traps emptied at the temperature T. A trap distribution function, $H(T)$, can be determined in arbitrary units as:

$$H(T) \propto \frac{I}{\mathrm{d}\langle E \rangle / \mathrm{d}T}, \quad (2)$$

where I is TSL after converting the temperature scale to the energy scale by means of empirically accessible dependence equation (1).

The conventional steady-state photoluminescence (PL) (continuous wave, cw-PL) was measured at temperatures ranging from 4.2 K to 300 K using an optical helium cryostat. All PL spectra were corrected for background radiation and instrumental spectral response. The studied organic films did not exhibit any notable photo-degradation during the measurements.

3 Results and discussion

3.1 Photoluminescence spectroscopy studies

Figure 2 shows steady-state PL spectra of the ionic perylene derivative Per-2582SL and the neutral derivative PTCDI-C5. PL spectra of Per-2582SL (Fig. 2a) were measured in aqueous solution ($c = 10^{-5}$) at room temperature (curves 1) as well as in a solid film at 5 K (curves 2) and at room temperature (curves 3). For comparison purposes, Figure 2b shows PL spectra of PTCDI-C5 measured in tetrahydrofuran (THF) solution at room temperature (curve 1), and in a film at 5 K and 300 K (curves 2 and 3, respectively). The PL intensity in Per-2582SL was considerably weaker as compared to that of PTCDI-C5 when measured under the same experimental conditions, that implies much smaller PL yield in this material. The PL spectrum of PTCDI-C5 in diluted THF solution features a 0-0 transition at 537 nm (Fig. 2b) that is almost in resonance with the lowest energy absorption band at 527 nm (not shown here), and therefore it could be attributed to emission from isolated molecules diluted in the solvent. The 0-0 PL transition of Per-2582SL in solution is observed in almost the same spectrum range at around 547 nm, which implies that energy levels of the lowest excited state of these compounds are not much altered by different periphery groups and by the presence of ions.

Note that PL spectrum in PTCDI-C5 film is greatly shifted (by ∼0.45 eV) to a longer wavelength (∼665 nm) with respect to the spectrum for diluted solution (Fig. 2b)

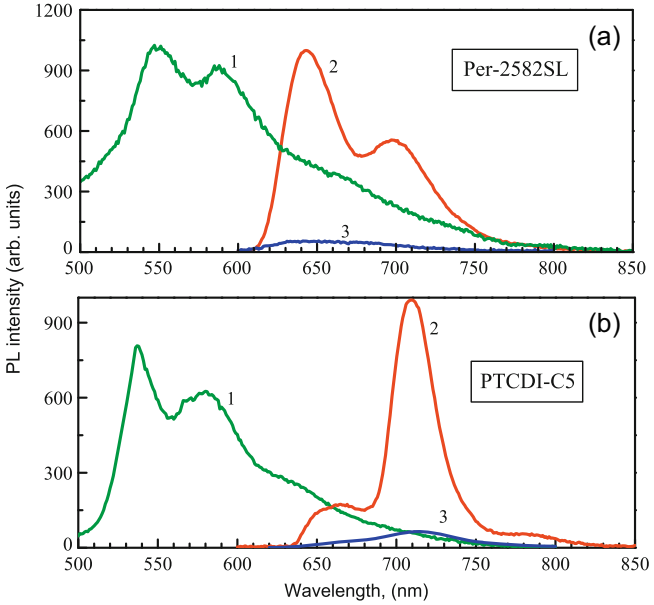

Fig. 2. PL spectra of the perylene derivatives: (a) Per-2582SL and (b) PTCDI-C5 measured in solution ($c = 10^{-5}$) (curves 1) at room temperature, and in solid films at 5 K (curves 2) and room temperature (curves 3).

that is an evidence for enhanced intermolecular coupling in the films. The strong bathochromic shift of PL spectra (by ∼0.33 eV) from diluted solution to solid film is also observed in ionic Per-2582SL (Fig. 2a), which imply similarly strong intermolecular interaction in aggregates of LCLC solid films. The latter behavior is expected to be favorable for the charge-carrier transport in such materials due to enhanced wavefunction overlap between neighboring molecules, that makes them promising for application in electronic devices.

Temperature dependent PL spectra measured in Per-2582SL and PTCDI-C5 solid films are shown in Figure 3. PL intensity for both compounds strongly decreases with increasing temperature from 5 K to room temperature, and the shape of PL spectra changes considerably. The PL spectrum of PTCDI-C5 film at 5 K features three peaks at ∼665 nm, ∼710 nm and ∼785 nm, while a very broad emission band peaking at 715 nm dominates the PL spectra at room temperature (Fig. 3b). Basically similar PL properties have been reported for films of other perylene diimide derivatives [41,42] where the latter broad peak was ascribed either to emission from excimer-type species or to emission from self-trapped excitons. The pronounced PL band at around 715 nm in PTCDI-C5 films is related to a low-energy state in this material which might be responsible for not only the exciton trapping but also for a moderately deep charge-carrier trapping, as it will be shown in successive section. PL spectra of Per-2582SL also decrease in intensity with elevating temperature (Fig. 3a), however, their shapes do not change so considerably as the temperature-dependent spectra of PTCDI-C5 (Fig. 3b). The fact that such low-energy PL band (especially at room temperature) is much less pronounced in Per-2582SL films might imply a smaller concentration of gap states in this

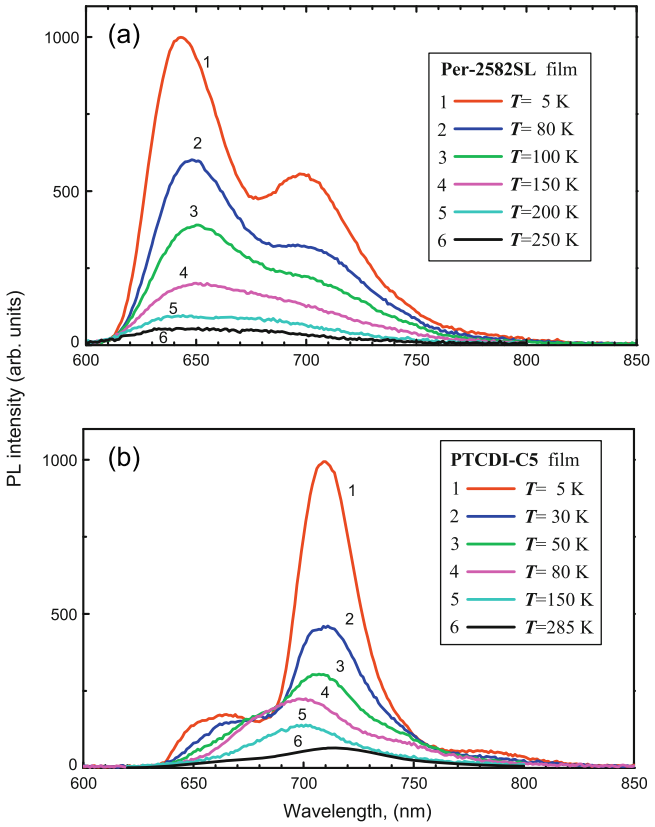

Fig. 3. PL spectra of solid films of (a) Per-2582Sl and (b) PTCDI-C5 measured at different temperatures under excitation with $\lambda_{exc} = 365$ nm.

material. This might be a consequence of liquid-crystalline morphology of Per-2582SL films.

3.2 Thermally stimulated luminescence study

A typical TSL glow curve of a Per-2582SL film (deposited from aqueous solution) measured after excitation with 365 nm-light for a few min at 4.2 K is shown in Figure 4 (curve 1). The TSL of a PTCDI-C5 film measured under the same conditions is given for comparison (Fig. 4, curve 2). Up to our knowledge, TSL was never reported before for perylene diimide derivative materials. The TSL of Per-2582SL film reveals a broad slightly asymmetric peak with the maximum at around $T_m \approx 50$ K and the TSL signal is detected only at relatively low-temperatures ($T < 200$ K) as expected for a disordered material devoid of deep charge-carrier trapping. The observed low-temperature TSL peak can be ascribed to detrapping of charge carriers from shallow localized states.

As evident from Figure 4, there is a remarkable difference between the TSL curves of Per-2582SL and PTCDI-C5 films. The TSL curve of PTCDI-C5 has a different shape, namely, apart of the low-temperature peak at about 30 K it shows also a distinct additional TSL band peaking at ~110 K. Dotted lines in Figure 4 show a deconvolution of the experimental curve into two Gaussian-shaped peaks. The TSL peak at 110 K seems to be an

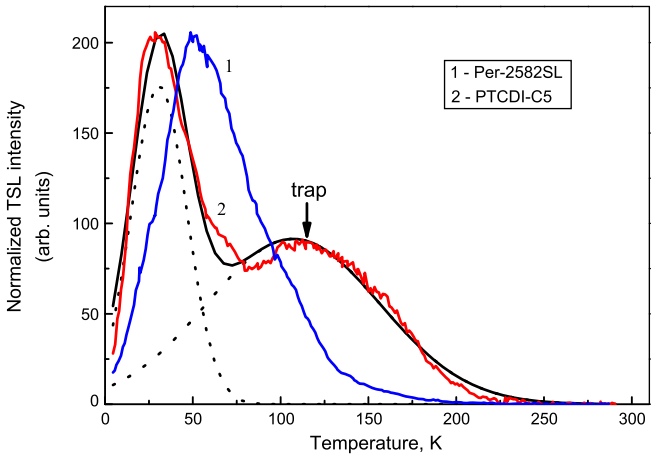

Fig. 4. TSL glow curves of Per-2582SL and PTCDI-C5 film (curves 1 and 2, respectively) after excitation with 365 nm light at 4.2 K. The TSL curves are normalized to the maximum intensity. Doted lines show a deconvolution of the experimental curve for PTCDI-C5 film into two Gaussian-shaped peaks and the black solid curve is used to fit the experimental data with bimodal Gaussian distribution.

inherent feature of PTCDI-C5 films and it implies the presence of moderately deep extrinsic charge-carrier trap responsible for this peak. These trap states are seemingly inherent for this material since our attempts to prepare a film devoid of the additional 110 K peak failed. Similar TSL phenomena have been observed in other organic semiconductors we studied before [28–33]. The observed trap states form an additional DOS distribution shifted to deeper energies with respect to the main Gaussian DOS of charge transport states. Thus, overlapping of both distributions yields a bimodal cumulative DOS distribution [28] characteristic for the PTCDI-C5 films.

3.3 TSL data analysis

The observed characteristic features of TSL presented above can be explained in terms of the hopping model for thermally assisted relaxation in disordered organic materials [28,31], which permits the evaluation of the DOS distribution from the TSL data. According to the model, TSL arises from radiative recombination of sufficiently *long geminate pairs* of charge-carriers created during photoexcitation of the sample at a low (helium) temperature. The long-range off-chain geminate charge pairs could be stable enough against isothermal recombination at cryogenic temperatures (note that TSL is not changed after the sample was stored at 4.2 K for many hours) provided that the constituting charge-carriers are trapped by sufficiently deep localized states. The latter could be intrinsic hopping states localized within the tail of the DOS or extrinsic trap states of different origin. It was shown that the deepest portion of an energetically disordered manifold of localized states could be responsible for shallow charge trapping at very low temperatures [28] in trap-free systems, while extrinsic traps can cause moderate

or deep charge trapping in trap-containing materials. It worth mentioning that recent combining TSL and thermally stimulated current (TSC) studies in the same materials [43] have demonstrated that the Coulomb binding energy in the photogenerated charge pairs does not really affect the TSL data, however, it can change considerably TSC curve and the apparent activation energy of TSC due to the Coulomb interaction impedes dissociation of charge pairs into free charge carriers contributing to conductivity [44]. Concomitantly, the analysis of a TSL curve directly yields information about the DOS distribution [43,44]; and the energy distribution of trapped carriers obtained from TSL data is an exact replica of the deeper portion of the DOS distribution [28,31].

In our previous studies of the TSL phenomena in trap-free disordered solids [28,31] we have proved that the high-temperature tail of a TSL curve becomes a straight line when plotted on a $\log(I_{\mathrm{TSL}})$ vs. T^2 scale or $\log(I_{\mathrm{TSL}})$ vs. $\langle E_a \rangle^2$ after converting the temperature scale to a trap energy scale by using a calibration equation related the mean activation energy $\langle E_a \rangle$ to temperature, that is measured by Fractional TSL technique. The slope of this line is a measure of the DOS width and yields the energy disorder parameter σ in the disordered organic material under study since it was demonstrated [28] that the high-temperature wing of the TSL curve is an exact replica of the deeper portion of the DOS distribution. This approach is conceptually similar to that employed earlier [45,46] using the thermally stimulated current (TSC) technique. Analysis of the shape of the high-energy wing of the TSC was used to determine the width of the DOS distribution in disordered layers of tetracene and pentacene.

A single TSL peak observed in Per-2582SL films suggests that a single-modal Gaussian DOS distribution is an appropriate approximation for this system and the above mentioned analysis is applicable. Owing to the relatively weak TSL signals in this material it was practically impossible to apply the fractional TSL techniques. However, as we found in our previous studies, the above empirical calibration equation varies not significantly for various disordered organic materials [31–33] unless the charger transporting sites are diluted as in molecularly doped polymers at low concentration of charge transport molecules [32], therefore the best we could do is to use the calibration equation obtained in our previous works: $\langle E_a \rangle (T) = 0.0018 \times T - 0.016$ (in eV) [28]. This empirical expression for $\langle E_a \rangle (T)$ in fact supports the basic formula of Simmons-Taylor theory [47] developed long ago for TSC, which predicts a qualitatively similar linear temperature dependence of the apparent activation energy. It worth noting that such kind of equation has been recently justified by the relevant analytical variable-range-hopping calculations for organic materials [31].

The results of Gaussian analysis of the high-temperature wing of the TSL peak of Per-2582SL and PTCDI-C5 film are presented in Figure 5 (curves 1 and 2, respectively). The high-temperature tails of TSL glow curves can be reasonably well approximated by straight lines and the width of the DOS distribution as estimated from its slope is 0.09 eV and 0.13 eV for Per-2582SL and

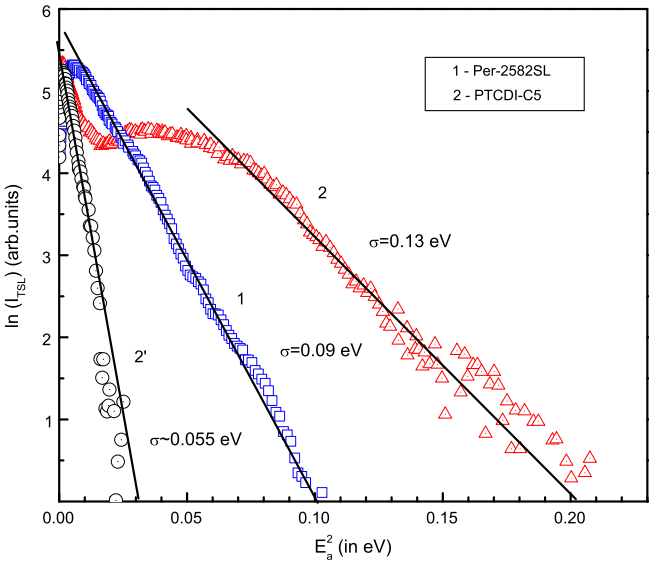

Fig. 5. Gaussian analysis of the high-energy wing of the TSL peak of a Per-2582SL (curve 1) and PTCDI-C5 (curve 2) films assuming that the deep tail states' distribution can be approximated by a Gaussian function $H(E) \propto \exp[-E^2/2\sigma^2]$. Curve 2′ presents analysis of the first TSL peak at 30 K of PTCDI-C5 separated by subtracting the second TSL peak at 110 K from the experimental TSL curve assuming on that the second (trap related) peak has a Gaussian profile shown by dotted curve in Figure 4. Estimated effective DOS widths are presented in the figure.

PTCDI-C5, respectively. Such values are quite typical for organic semiconducting films. It should be mentioned that in the above analysis it was assumed that the effective transport energy level coincides with the center of the DOS distribution [28]. The validity of such approximation for ordered and polycrystalline organic films have been presented before [34].

It should be mentioned that due to the TSL curve of PTCDI-C5 film consists of two distinct overlapping peaks, the estimated disorder parameter $\sigma = 0.13$ eV is largely determined by the second trap-related peak at 110 K, that seems to be quite natural for a trap containing material. Because of the lack of direct experimental access to the high-temperature wing of the first peak at 30 K, the above analysis method cannot be readily applied to this peak. However, to circumvent this issue one might separate the first peak by subtracting the second peak from the experimental TSL curve assuming that the second peak has a Gaussian profile as shown by dotted curve in Figure 4. This allows at least rough evaluation of the width of the DOS distribution related to the first peak. Curve 2′ in Figure 5 presents the Gaussian analysis of the first TSL peak separated in such way and its slope yields $\sigma \approx 0.055$ eV. This value is very similar to that determined before for a trap-free methyl-substituted ladder-type poly(paraphenylene) (MeLPPP) film [28] and could be considered as a rough estimate for the width of the intrinsic (trap-free) DOS distribution in PTCDI-C5 film.

The results of the above comparative TSL investigations of Per-2582SL and PTCDI-C5 can be understood in the following way.

- Firstly, the low-temperature TSL band observed in thin films of Per-2582SL implies mostly a shallow charge trapping due to the tail states of the intrinsic DOS distribution (which might certainly be affected by some shallow traps) and the deep intrinsic traps are negligible. As a result, the moderately low energetic disorder ($\sigma = 0.09$ eV) in this material along with the strong intermolecular coupling can explain the relatively high charge mobility we observed recently in this material.
- Secondly, in contrast to Per-2582SL, thin films of PTCDI-C5 clearly show the presence of fairly deep extrinsic traps with average depth around $E_{\rm trap}^{\rm charge} = 0.3$ eV, i.e., a clear bi-modal DOS distribution is realized, (Fig. 4, curve 2). Interestingly, that the observed extrinsic trap in TSL of PTCDI-C5 films correlates with the observation of pronounced excimer-type band in PL spectra of this material (Fig. 3). It is known that excimer-forming site can act as a charge-carrier trap as it was well documented e.g., in poly-vinylcarbazole polymers [48]. "Sandwich"-like excimers characterized by a coplanar arrangement of two neighboring carbazole units which is energetically favorable for charge trapping. Well-ordered LC morphology of Per-2582SL films results in reduction of both excimer-type PL emission and negligible deep charge-carrier trapping. Thus, PTCDI-C5 material is effectively more energetically disordered due to presence of moderately deep traps. The analysis of the high-temperature wind of the TSL curve of PTCDI-C5 (Fig. 5, curve 2) yields $\sigma \approx 0.13$ eV. The larger effective energy disorder in PTCDI-C5 films can easy be noticed even from TSL curves presented in Figure 4 as the overall TSL curve of PTCDI-C5 is notably extended to higher temperatures in comparison to that of Per-2582SL implying the presence of deeper states in the gap.
- Thirdly, the effect of the traps can be accounted for by introduction of the so-called "effective disorder parameter" $\sigma_{\rm eff}$ for a trap-containing disordered material. We showed by analytical calculations using an effective medium approximation (EMA) theory that this parameter at arbitrary relative trap concentration $0 \leq c \leq 1$, where $c = N_{\rm trap}/N$ is the ratio of trap sites $N_{\rm trap}$ to the total number of localized sites N in a material, can be obtained as [29].

$$\left(\frac{\sigma_{\rm eff}}{\sigma_0}\right)^2 = 1 + 2\left(\frac{k_{\rm B}T}{\sigma_0}\right)^2 \times \ln\left\{\frac{1 + c\exp\left[\frac{E_t}{k_{\rm B}T} + \frac{1}{2}\left(\frac{\sigma_0}{k_{\rm B}T}\right)^2\right]}{1 + c^2\exp\left[\frac{E_t}{k_{\rm B}T} + 2\frac{a}{b}\left(1 - \frac{1}{c^{1/3}}\right)\right]}\right\}, \quad (3)$$

where E_t trap depth, σ_0 is the width of the intrinsic DOS (trap-free DOS), a/b is the ratio between average intermolecular distance and localization radius of the charge carrier. Here it was assumed that the widths of intrinsic- and trap- DOS distributions are the same. Depending on the trap concentration, a different value of the $\sigma_{\rm eff}$ can be obtained. The physical reason for the effective disorder is that intrinsic DOS distribution overlaps with the trap distribution, so the cumulative DOS can be broader. This is confirmed by our TSL measurements in PTCDI-C5 films, which provide an estimate of the σ-parameter as 0.13 eV.

We should note that the effective disorder parameter $\sigma = 0.13$ eV estimated from the TSL data for PTCDI-C5 films is in perfect agreements with the data obtained before for this material by the charge transport measurements [38]. Indeed, the OFET mobility measurements in PTCDI-C5 films have revealed that thermally activated charge-carrier mobilities manifest the so-called Meyer-Neldel behavior when measured at different gate voltages, i.e., there is a well-defined isokinetic temperature ($T_{\rm MN}$) at which Arrhenius plots at different gate voltages intersect and the Meyer-Neldel energy $E_{\rm MN} = kT_{\rm MN} = 0.054$ eV was found for these films [38]. Recently it was demonstrated that the Meyer-Neldel energy $E_{\rm MN}$ in organic semiconductors is directly related to the width of the Gaussian DOS, σ, as $E_{\rm MN} = \frac{2}{5}\sigma$ [49], providing thus a method for evaluation of the amount of the energetic disorder in the material. The experimentally measured $E_{\rm MN} = 0.054$ eV [38] in PTCDI-C5 films yields $\sigma = 0.135$ eV, that agrees nicely with the parameter $\sigma = 0.13$ eV determined in the present study (Fig. 5) and justify the validity of the TSL method for evaluation of the energy disorder in perylene derivative based materials.

The above TSL study allows one to make an important conclusion - ionic LCLC films of Per-2582SL are *effectively* less energetically disordered compared to conventional PTCDI-C5 films deposed from solution (estimated disorder parameters are 0.09 eV vs. 0.13 eV, respectively), so the former should potentially be better charge transporting material and, consequently, more attractive for electronic device applications. We should, however, make a reservation that PTCDI-C5-based devices are conventionally fabricated by vacuum deposition method that could result in very different film morphology than that obtained by solution-based processing.

Let us discuss the reason why the effective disorder in Per-2582SL films could be smaller than in PTCDI-C5 ones. The effect is definitely related to different film morphology which is evidently more preferential in the LCLC films. The observed fairly deep charge-carrier trap in PTCDI-C5 films (Fig. 4) has most probably a structure-related origin that agrees with similar observations in other small molecule solids studied before [28,30,34]. From literature data it is known that PTCDI-C5 films deposited from solution contains some crystallites/aggregated regions that are surrounded by rather amorphous regions. Molecules in the aggregates are much stronger coupled and more ordered, so the LUMO and HOMO levels of aggregates are shifted to lower and higher energies, respectively, with respect to that of non-aggregate regions. The latter

conclusion is clearly supported by our PL studies presented in Figure 2b demonstrating that PL band responsible for the aggregates in PTCDI-C5 is shifted by 0.13 eV with respect to non-aggregated PL. In other words, aggregates act as traps for charge carriers as their energetic is favorable for that and thermal excitation of the charge-carriers back to amorphous region require overcoming energetic barrier formed by the mismatch in the corresponding HOMO/LUMO levels [50]. The latter is just responsible for the structure-related trap with depth of $E_{\rm trap}^{\rm charge} = 0.3$ eV observed in our TSL experiment. It is well known that structure-related defects in organic materials should create traps for both excitons and charge carriers due to enhanced electronic polarization at such defect state. Previous theoretical calculations [51,52] showed that the trap for charge carriers should be approximately 2–3 times deeper than the exciton trap on the same structural defect [51]. This indeed seems to occur in PTCDI-C5 films where the charge trap is of 0.3 eV depth while the exciton trap is by 0.13 eV shifted with respect to the 0-0 PL exciton transition (Fig. 2b).

Absence of such fairly deep trap in Per-2582SL films does not imply the absence of aggregated regions in them, but on the contrary it evidences that aggregated regions become dominated in this material and their concentration is large enough to form quite extended regions (called also as conductive channels). Possible amorphous regions play no essential role anymore. Therefore, the energy disorder parameter obtained by TSL in Per-2582SL films characterize just the dominated well ordered aggregated regions since all charge carriers eventually sink into the latter places. Indeed, as we showed recently the conductive channels of macroscopic length are formed due to self-assembling of LCLC molecules in aggregates in solution phase, which are then transported into the solid films.

4 Conclusions

We obtained direct evidence by TSL technique for the improved energetic ordering (smaller effective energetic disorder parameter) in aggregated LCLC films as compared to films of chemically-similar PTCDI-C5. Effective disorder parameters $\sigma = 0.09$ eV and 0.13 eV were estimated for Per-2582SL and PTCDI-C5, respectively. For the latter material, the disorder parameter was found to be in perfect agreement with that determined from previous temperature-dependent charge transport measurements. The formation of macroscopically large LCLC aggregates is responsible for relatively smaller effective energetic disorder in Per-2582SL and these aggregates provide percolative (conductive) passes for charge carriers in such films. In contrast, the aggregates formed in PTCDI-C5 films are of smaller size and in lower concentration surrounded by amorphous regions, so they play a role of fairly deep traps ($E_{\rm trap}^{\rm charge} = 0.3$ eV) as their concentration is not always sufficient to form percolation pass. The width of intrinsic (trap-free) DOS distribution for PTCDI-C5 films was estimated as $\sigma \approx 0.055$ eV.

The authors thank Taras Turiv for assistance with experimental measurements and Prof. V. Gulbinas for helpful discussions. OPB acknowledges support from the Research Council of Lithuania – Project No. VP1-3.1-SMM-01-V-02-004 (Postdoctoral Fellowship). This work was supported by NSF Materials World Network on Lyotropic Chromonic Liquid Crystals (Project #DMR076290), by the Science and Technology Center in Ukraine (Project #5258), by National Academy of Science of Ukraine (Project #1.4.1B/10) and by the European Research Council via Grant # 320680 (EPOS CRYSTALLI).

References

1. H. Klauk, *Organic Electronics: Materials, Manufacturing and Applications* (Wiley-VCH, Weinheim, 2006)
2. M. Berggren, D. Nilsson, N.D. Robinson, Nat. Mater. **6**, 3 (2007)
3. H. Bässler, Phys. Stat. Sol. B **175**, 15 (1993)
4. T.W. Kelley, D.V. Muyres, P.F. Baude, T.P. Smith, T.D. Jones, Mater. Res. Soc. Symp. Proc. **771**, L6.5 (2003)
5. V.I. Arkhipov, I.I. Fishchuk, A. Kadashchuk, H. Bässler, in *Semiconducting Polymers: Chemistry, Physics and Engineering*, Vol. I, 2nd edn., edited by G. Hadziioannou, G.G. Malliaras (Wiley-VCH Verlag GmbH & Co. KGaA, Weinheim, 2007), p. 275
6. P.M. Borsenberger, D.S. Weiss, *Organic Photoreceptors for Xerography* (Marcel Dekker, NY, 1998)
7. S. Nespurek, J. Pfleger, E. Brynda, I. Kmínek, A. Kadashchuk, A. Vakhnin, J. Sworakowski, Mol. Cryst. Liq. Cryst. **355**, 191 (2001)
8. J. Takeya, J. Kato, K. Hara, M. Yamagishi, R. Hirahara, K. Yamada, Y. Nakazawa, S. Ikehata, K. Tsukagoshi, Y. Aoyagi, T. Takenobu, Y. Iwasa, Phys. Rev. Lett. **98**, 196804 (2007)
9. T. Hasegawa, J. Takeya, Sci. Technol. Adv. Mater. **10**, 024314 (2009)
10. A.L. Briseno, S.C.B. Mannsfeld, M.M. Ling, S. Liu, R.J. Tseng, C. Reese, M.E. Roberts, Y. Yang, F. Wudl, Z. Bao, Nature **444**, 913 (2006)
11. H. Minemawari, T. Yamada, H. Matsui, J. Tsutsumi, S. Haas, R. Chiba, R. Kumai, T. Hasegawa, Nature **475**, 364 (2011)
12. A. Andreev, G. Matt, C.J. Brabec, H. Sitter, D. Badt, H. Seyringer, N.S. Sariciftci, Adv. Mater. **12**, 629 (2000)
13. H. Yanagi, T. Morikawa, Appl. Phys. Lett. **75**, 187 (1999)
14. B. Müller, T. Kuhlmann, K. Lischka, H. Schwer, R. Resel, G. Leising, Surf. Sci. **418**, 256 (1998)
15. F. Balzer, H.G. Rubahn, Appl. Phys. Lett. **79**, 3860 (2001)
16. C. Simbrunner, F. Quochi, G. Hernandez-Sosa, M. Oehzelt, R. Resel, G. Hesser, M. Arndt, M. Saba, A. Mura, G. Bongiovanni, H. Sitter, ACS Nano **4**, 6244 (2010)
17. I. McCulloch, W. Zhang, M. Heeney, C. Bailey, M. Giles, D. Graham, M. Shkunov, D. Sparrowe, S. Tierney, J. Mater. Chem. **13**, 2436 (2003)

18. A. Demenev, S.H. Eichhorn, T. Taerum, D.F. Perepichka, S. Patwardhan, F.C. Grozema, L.D.A. Siebbeles, R. Klenkler, Chem Mater. **22**, 1420 (2010)
19. V.G. Nazarenko, O.P. Boiko, M.I. Anisimov, A.K. Kadashchuk, Yu.A. Nastishin, A.B. Golovin, O.D. Lavrentovich, Appl. Phys. Lett. **97**, 263305 (2010)
20. V.G. Nazarenko, O.P. Boiko, H.S. Park, O.M. Brodyn, M.M. Omelchenko, L. Tortora, Yu.A. Nastishin, O.D. Lavrentovich, Phys. Rev. Lett. **105**, 017801 (2010)
21. J.E. Lydon, Curr. Opin. Colloid Interface Sci. **8**, 480 (2004)
22. K.V. Kaznatcheev, P. Dudin, O.D. Lavrentovich, A.P. Hitchcock, Phys. Rev. E **76**, 061703 (2007)
23. Yu.A. Nastishin, H. Liu, T. Schneider, V. Nazarenko, R. Vasyuta, S.V. Shiyanovskii, O.D. Lavrentovich, Phys. Rev. E **72**, 041711 (2005)
24. L. Ignatov, P. Lazarev, V. Nazarov, N. Ovchinnikova, M. Paukshto, Proceedings SPIE: Phys. Chem. Interfaces Nanomater. **4807**, 177 (2002)
25. R. Schmechel, H. Seggern, Phys. Stat. Sol. A **201**, 1215 (2004)
26. A. Kadashchuk, R. Schmechel, H. Seggern, U. Scherf, A. Vakhnin, J. Appl. Phys. **98**, 024101 (2005)
27. I. Glowacki, Z. Szamel, J. Phys. D: Appl. Phys. **43**, 295101 (2010)
28. A. Kadashchuk, Yu. Skryshevskii, A. Vakhnin, N. Ostapenko, V.I. Arkhipov, E.V. Emelianova, H. Bässler, Phys. Rev. B **63**, 115205 (2001)
29. I.I. Fishchuk, A.K. Kadashchuk, A. Vakhnin, Yu. Korosko, H. Bässler, B. Souharce, U. Scherf, Phys. Rev. B **73**, 115210 (2006)
30. A. Kadashchuk, Yu. Skryshevskii, Yu. Piryatinski, A. Vakhnin, E.V. Emelianova, V.I. Arkhipov, H. Bässler, J. Shinar, J. Appl. Phys. **91**, 5016 (2002)
31. V.I. Arkhipov, E.V. Emelianova, A. Kadashchuk, H. Bässler, Chem. Phys. **266**, 97 (2001)
32. A. Kadashchuk, D.S. Weiss, P.M. Borsenberger, S. Nešpurek, N. Ostapenko, V. Zaika, Chem. Phys. **247**, 307 (1999)
33. A. Kadashchuk, N. Ostapenko, V. Zaika, S. Nespurek, Chem. Phys. **234**, 285 (1998)
34. A. Kadashchuk, A. Andreev, H. Sitter, N.S. Sariciftci, Yu. Skryshevskii, Yu. Piryatinski, I. Blonsky, D. Meissner, Advan. Func. Mater. **14**, 970 (2004)
35. T. Schneider, K. Artyushkova, J.E. Fulghum, L. Broadwater, A. Smith, O.D. Lavrentovich, Langmuir **21**, 2300 (2005)
36. K. Misawa, H. Ono, K. Minoshima, T. Kobayashi, Appl. Phys. Lett. **63**, 577 (1993)
37. O.P. Boiko, R.M. Vasyuta, V.G. Nazarenko, V.M. Pergamenshchik, Yu.A. Nastishin, O.D. Lavrentovich, Mol. Cryst. Liq. Cryst. **467**, 181 (2007)
38. R.J. Chesterfield, J.C. McKeen, C.R. Newman, P.C. Ewbank, D.A. da Silva Filho, J.L. Bredas, L.L. Miller, K.R. Mann, C.D. Frisbie, J. Phys. Chem. B **108**, 19281 (2004)
39. Th.B. Singh, S. Erten, S. Günes, C. Zafer, G. Turkmen, B. Kuban, Y. Teoman, N.S. Sariciftci, S. Icli, Org. Electr. **7**, 480 (2006)
40. T. Mori, J. Phys.: Condens. Matter **20**, 184010 (2008)
41. H.P. Wagner, A. DeSilva, T.U. Kampen, Phys. Rev. B **70**, 235201 (2004)
42. A.J. Ferguson, T.S. Jones, J. Phys. Chem. B **110**, 6891 (2006)
43. A. Kadashchuk, A. Vakhnin, H. von Seggern, U. Scherf, Ukr. J. Phys. **54**, 68 (2009)
44. V.I. Arkhipov, E.V. Emelianova, R. Schmechel, H. von Seggern, J. Non-Cryst. Solids **338**, 626 (2004)
45. H. Bässler, Phys. Stat. Sol. B **107**, 9 (1980)
46. R. Eiermann, W. Hofberger, H. Bässler, J. Non-Cryst. Solids **28**, 415 (1978)
47. J.G. Simmons, G.W. Taylor, Phys. Rev. B **5**, 1619 (1972)
48. H. Ohkita, Y. Nomura, A. Tsuchida, M. Yamamoto, Chem. Phys. Lett. **263**, 602 (1996)
49. I.I. Fishchuk, A. Kadachchuk, J. Genoe, Mujeeb Ullah, H. Sitter, Th.B. Singh, N.S. Sariciftci, H. Bässler, Phys. Rev. B **81**, 045202 (2010)
50. A.J. Mozer, P. Denk, M.C. Scharber, H. Neugebauer, N.S. Sariciftci, P. Wagner, L. Lutsen, D. Vanderzande, A. Kadashchuk, R. Staneva, R. Resel, Synth. Met. **153**, 81 (2005)
51. E.A. Silinsh, *Organic Molecular Crystals. Their Electronic States* (Springer-Verlag, Berlin, 1980)
52. M. Pope, C.E. Swenberg, *Electronic Processes in Organic Crystals and Polymers*, 2nd edn. (Oxford University Press, Oxford, 1999)